Journal of Materials Physics and Chemistry, 2024, Vol. 12, No. 1, 1-10
Available online at http://pubs.sciepub.com/jmpc/12/1/1
Published by Science and Education Publishing
DOI:10.12691/jmpc-12-1-1

Gravimetric and Quantum Chemical Approach of Nifuroxazid as Inhibitor of Aluminium Corrosion In 2.0 M HCl

Cissé M'bouillé[1,*], Mougo André Tigori[1], Assoman Kouakou Alain[1], Amadou Kouyaté[1], Paulin Marius Niamien[2]

[1]Laboratoire des Sciences et Technologies de l'Environnement, UFR Environnement,
Université Jean Lorougnon Guédé, Daloa, Côte d'Ivoire
[2]Laboratoire de Constitution et de Réaction de la Matière, UFR SSMT,
Université Félix Houphouët-Boigny, Abidjan, Côte d'Ivoire
*Corresponding author: mbouille.cisse07@gmail.com

Received January 20, 2024; Revised February 22, 2024; Accepted March 02, 2024

Abstract Corrosion is a phenomenon that needs to be monitored with great care, as it is becoming more widespread in many areas. The present work was carried out to test 4-hydroxy-N-[(5-nitrofuran-2-yl) methylene] or nifuroxazid as a corrosion inhibitor for aluminium corrosion in 2M HCl. This work was evaluated by mass loss technique and quantum chemical calculations. The results show that this compound has a good inhibition capacity in medium studied. Compound inhibition efficiency decreases with increasing temperature, while increasing compound concentration is accompanied by a decrease in corrosion rate and thus an increase in inhibition efficacy. Isotherms adsorption study shows that inhibitor adsorbs on aluminium surface according to the modified Langmuir model. Thermodynamic values for adsorption and activation show that adsorption is spontaneous and exothermic, with an increase in disorder. The adsorption process was found to combine chemical and physical adsorption, with physisorption predominating. The mechanism of inhibition was explained by quantum chemical parameters derived from density functional theory (DFT) calculations, and reactivity sites determination which to identify electrophilic and nucleophilic centers of attack.

Keywords: *nifuroxazid, corrosion, aluminium, mass loss technique, density functional theory*

Cite This Article: Cissé M'bouillé, Mougo André Tigori, Assoman Kouakou Alain, Amadou Kouyaté, and Paulin Marius Niamien, "Gravimetric and Quantum Chemical Approach of Nifuroxazid as Inhibitor of Aluminium Corrosion In 2.0 M HCl." *Journal of Materials Physics and Chemistry*, vol. 12, no. 1 (2024): 1-10. doi: 10.12691/jmpc-12-1-1.

1. Introduction

Because of its superior mechanical and chemical qualities, aluminium and its alloys are often employed in a broad domain of technical and technological processes, such as automobiles, household appliances, aluminium containers, electronic devices, building, aviation etc. The demands for long-term performance of engineering structures over a wide size scale continue to increase. Unfortunately, one of the biggest drawbacks of employing aluminium based alloys is that it is liable to corrosion [1,2,3,4]. Corrosion can be defined as the deterioration of a material's properties due to its interaction with its environment. Aluminium corrosion can be costly to industries and result in significant losses due to lost production, inefficient operation, and high maintenance. Aluminium corrosion is an inevitable but manageable phenomenon.

It has been found that one of the best methods of protecting metals against corrosion involves the use of inhibitors which are substances that slow down the rate of corrosion [5,6]. Therefore, the development of corrosion inhibitors based on organic compounds containing nitrogen, oxygen atoms is of growing interest in the field of corrosion and industrial applications [7]. Organic compounds are believed to reduce corrosion by adhering to metal surface. The steric effect, molecular weight, structure, solution temperature, and the metal/solution interface all have an impact on the adsorption in addition to the electron density at the donor site (aromatic rings and π-bonds) [8,9,10,11,12]. To address environmental demands, the use of organic inhibitors was suggested. Due to their toxicity, inorganic inhibitors (such as nitrites, chromates, silicates, phosphonates, and salts of zinc, cadmium and arsenic salts) which were broadly applied for many years in metals protection against corrosion, are avoided now [13].

Recently, several studies have been carried out on metals inhibition corrosion by drugs [14,15,16,17,18,19,20]. Moreover, the pharmaceutically active compounds are often big enough (molecular mass) and likely to effectively cover more surface area (due to adsorption) of aluminium. Furthermore, drugs are relatively cheap, easily available, and

environmentally friendly and most importantly is nontoxic. In view of these favourable characteristic properties, drugs were chosen for the corrosion studies [21,22].

Although experimental study provides information about the inhibitory efficacy of a compound in metal corrosion, a thorough understanding of the property and mechanism of inhibition remains of crucial interest. This is why theoretical methods have been introduced to explain the inhibition mechanism. Indeed, DFT, which includes electronic correlation in its formalism, provides a better explanation of metal-molecule interactions [23,24,25]. As a result, numerous studies in the literature [26,27,28,29,30,31] have reported the use of DFT calculations in the inhibition of aluminium corrosion in acidic media. It has been shown that the selection of effective corrosion inhibitors [32,33] is based on a good correlation between experimental and theoretical data.

The aim of this study is to examine the behaviour of 4-hydroxy-N-[(5-nitrofuran-2-yl)methylene]benzohydrazide or nifuroxazid for aluminium corrosion in 2M hydrochloric acid. Therefore, it is necessary to determine the adsorption capacity of this compound on aluminium surface, and reactivity sites involved in adsorption.

2. Material and Methods

2.1. Aluminium Samples Preparation

The aluminium samples were in the form of rod measuring 10mm in length and 2mm in diameter. The samples were polished with abrasive paper ranging from 150 to 600 grit, cleaned with acetone, washed with distilled water and dried in an oven. The samples were then weighed (m_1).

2.2. Solution Test Preparation

All reagents and solvents used in the experiment were of analytical grade and used without further purification. The aggressive solution of 2.0 M HCl was prepared by diluting the analytical grade 37% (Merck Chemicals) with distilled water. Acetone from Sigma Aldrich with purity: 99.5%. The inhibitor nifuroxazid (Figure 1) was acquired from Sinopharm chemical reagent. Four concentrations have been prepared from this inhibitor which are 1.45 mM, 3.63mM, 7.26 mM and 14.5 mM.

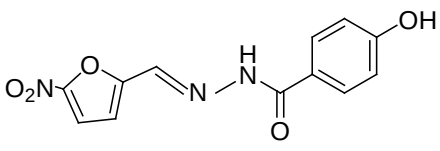

Figure 1. Chemical structure of Nifuroxazid

2.3. Gravimetric Details

After sample preparation, each sample was immersed in 50 ml of 2M HCl without or with different concentrations of nifuroxazid. A SELECTA water thermostat (FRIGITHERM) was used to maintain test solution temperatures from 298 to 328K. After 1 h, samples were removed, washed with distilled water, dried and weighed (m_2). All tests were carried out in aerated solutions. Mass losses were determined on the basis of three tests. The expressions below are used to determine the gravimetric quantities that are corrosion rates W, degree of surface coverage (θ) and inhibition efficiency (IE).

$$W = \frac{m_1 - m_2}{St} \quad (1)$$

Where m_1 and m_2 are respectively the mass before and after immersion in the test solution, S is the total surface of the sample and t is the immersion time.

$$IE(\%) = \frac{W_0 - W}{W_0} \times 100 \quad (2)$$

W_0 is the corrosion rate without the tested compound and W is the corrosion rate in presence of tested compound.

2.3. Quantum Chemical Assessment

In the present investigation, density functional theory (DFT) was used to explain nifuroxazid reactivity. This method, which stems from quantum chemistry, provides detailed information on the corrosion inhibition mechanism. Gravimetry provides access to compound studied inhibition efficiencies at different temperatures and concentrations, without explaining the metal-molecule interactions. In order to understand these interactions, DFT calculations were performed in gas phase using Gaussian 09 software package [34] was used with Becke's three parameter exchange functional along with the Lee-Yang-Parr B3LYP [35,36], on 6-31G(d, p) basis set. Parameters such as highest occupied molecular orbital energy (E_{HOMO}), lowest unoccupied molecular orbital energy (E_{LUMO}), energy gap (ΔE), dipole moment (μ), total energy (E_T), electron affinity (A), the ionization energy (I), electronegativity (χ), hardness (η), softness (σ) and electrophylicity index (ω) are related to ionization energy (I) and electron affinity (A), fraction of electrons transferred (ΔN) were calculated. Figure 2 shows nifuroxazid optimized structure in B3LYP/6-31G(d,p).

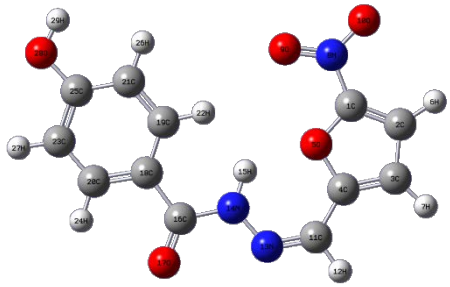

Figure 2. Nifuroxazid optimized structure with B3LYP/6-31G (d, p)

3. Results and Discussion

3.1. Gravimetric Consideration

3.1.1. Inhibitor Concentration and Temperature

The evolution of the corrosion rate versus temperature and concentration is shown in Figure 3 and Figure 4 indicates the inhibition efficiency variation as a function of temperature and inhibitor concentration.

Figure 3 reports clearly that corrosion rate in nifuroxazid absence is high, and that this rate increases with rising temperature, but is reduced as nifuroxazid concentration increases. With regard to Figure 4, inhibition efficiency decreases with increasing temperature and increases with increasing nifuroxazid concentration. These observations suggest that nifuroxazid presence in aggressive media creates a physical barrier capable of slowing down metal oxidation.

It can also be said that higher temperatures lead to weaker adsorption of nifuroxazid on metal surface, resulting in lower inhibition efficiencies at higher temperatures. In fact as the temperature rises, aluminium loses a lot of electrons, and nifuroxazid is unable to supply enough electrons to replace this loss when it is absorbed by metal surface, hence the drop in inhibition efficiency at high temperatures. While, increasing inhibitor concentration accelerates its adsorption to aluminium surface, which justifies the increase in inhibition efficiency as nifuroxazid concentration rises. Similar results have been observed in the literature with some phthalocyanine and thalocyanine deravatives and jasminum nudiflorum leaves extract [37,38,39,40].

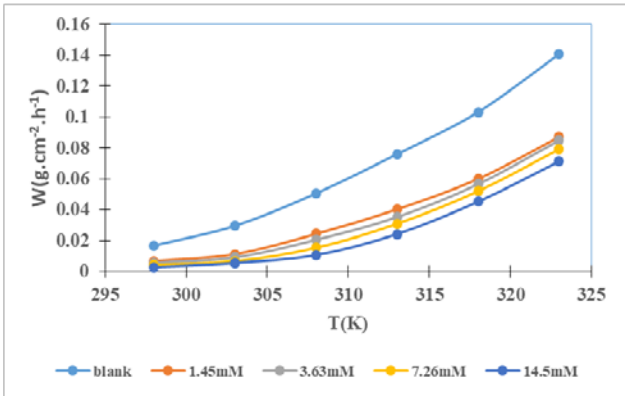

Figure 3. Corrosion rate versus temperature and nifuroxazid concentration

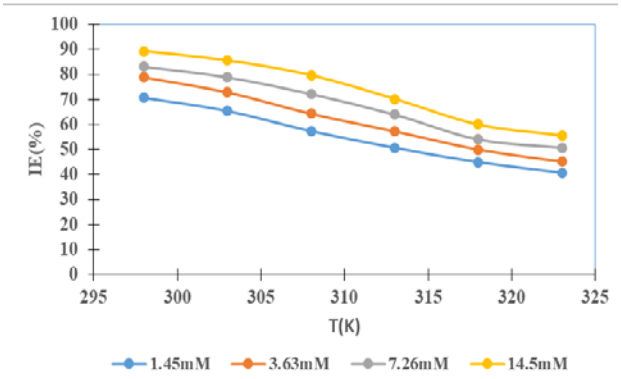

Figure 4. Inhibition efficiency vs. temperature for different concentrations in nifuroxazid

3.1.2. Adsorption Isotherm and Thermodynamic Adsorption Parameters Study

Heterogeneous reactions are generally understood through the study of adsorption isotherms. In fact, inhibition by organic molecules on the surface of a metal is governed by the adsorption process. The adsorption isotherms study involved in the process of metals corrosion inhibition by organic molecules allows to show how these compounds bind to the surface of a metal. The following relation [41] provides the general form of these isotherms.

$$f(\theta.x)\exp\exp(-g\theta) = K_{ads}C_{inh} \quad (3)$$

Where $f(\theta.x)$ is the configurational factor subject to the physical model and assumptions involved in the derivation of the isotherms. C_{inh} is the inhibitor concentration, θ is the surface coverage. K_{ads} is the equilibrium constant of the adsorption process and g is a parameter that expresses the interaction of the molecules in the adsorbed layer.

In this work we attempted various adsorption isotherms and selected those that better reflect Nifuroxazid behaviour on aluminium surface. So we have retained Langmuir, Temkin, El-Awady and Freundlich isotherms. The equations that define these isotherms are expressed in Table 1.

Table 1. Equations of studied isotherm

Isotherm	Equations
Langmuir	$\frac{C_{inh}}{\theta} = \frac{1}{K_{ads}} + C_{inh}$
Temkin	$\theta = \frac{2.303}{f}[logK_{ads} + logC_{inh}$
El-Awady	$log\left(\frac{\theta}{1-\theta}\right) = logK' + ylogC_{inh}$
Freundlich	$log\theta = logK_{ads} + nlogC_{inh}$

C_{inh} is nifuroxazid's concentration

K_{ads} is the equilibrium constant of the adsorption process

f is a factor of energetic inhomogeneity in the surface

θ is surface coverage

$$K_{ads} = K'^{1/y}$$

$1/y$ is active site occupied by inhibitor molecule.

Figure 5, Figure 6, Figure 7 and Figure 8 show the representation of these different isotherms. All the tested isotherms yield straight lines as shown in Figures.

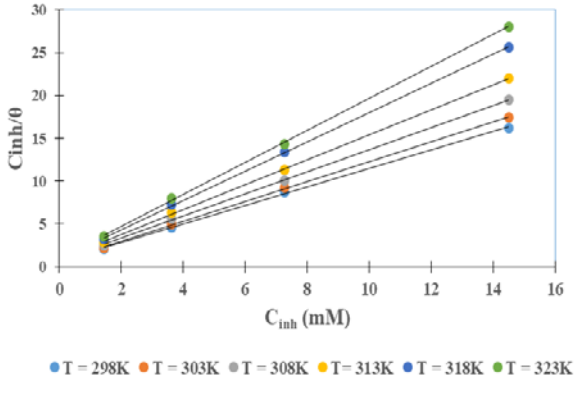

Figure 5. Langmuir adsorption isotherm plots of nifuroxazid on aluminium in 2M HCl

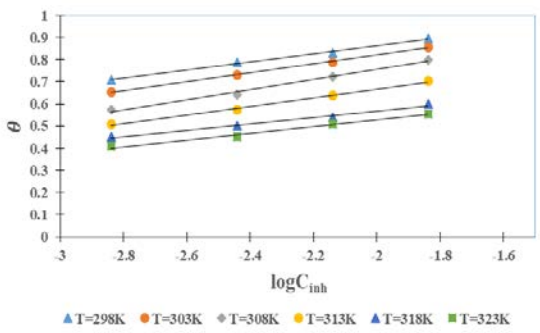

Figure 6. Temkin adsorption isotherm plots of nifuroxazid on aluminium in 2M HCl

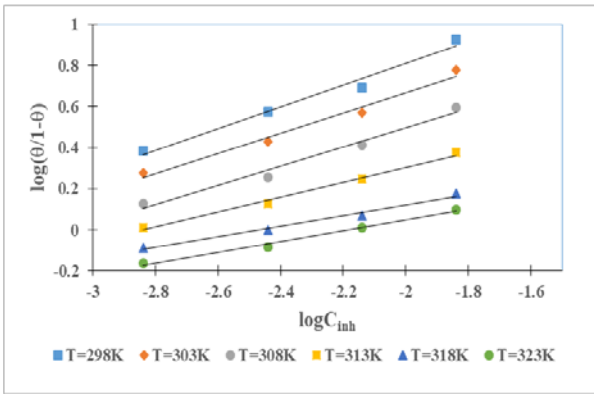

Figure 7. El-Awady adsorption isotherm plots of nifuroxazid on aluminium in 2M HCl

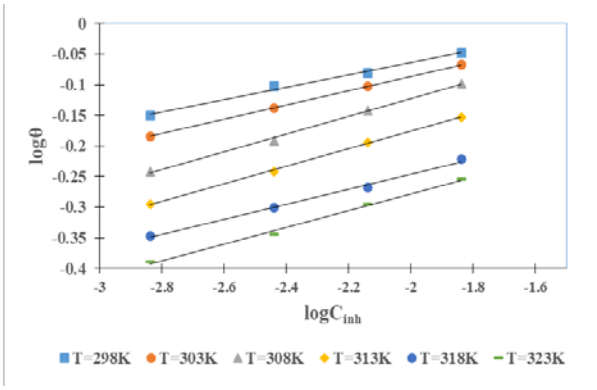

Figure 8. Freundlich adsorption isotherm plots of nifuroxazid on aluminium in 2M HCl

Table 2 gives the different parameters of studied isotherms. By looking the Table 2, it is clear that the correlation coefficients of Langmuir isotherm are closer to unity than the other isotherms. The deviation of the slopes from unity shows that this model cannot be applied rigorously. However, Temkin and El-Awady models can be applied. For Temkin model [41], the parameter f (where 2.303/f is the slope of straight lines) having a positive value, there would be repulsion forces between the molecules adsorbed on aluminium. As for El-Awady model [42], the inverse of the slopes (1/y) of the straight lines obtained is greater than unity, this means that a nifuroxazid molecule occupies more than one site. Langmuir adsorption model requires that the interactions between adsorbed particles are negligible and that each site can adsorb only one particle [43]. In this case, nifuroxazid adsorption on aluminium is not rigorously done according to Langmuir model; it is done according to the modified Langmuir isotherm or Villamil model [44]. This model represented by the equation:

$$\frac{C_{inh}}{\theta} = \frac{n}{K_{ads}} + nC_{inh} \qquad (4)$$

where C_{inh} represents the concentration of the inhibitor, θ is the surface area and K_{ads} is the adsorption equilibrium constant. The K_{ads} values were obtained by a linear straight fitted plot between $\frac{C_{inh}}{\theta}$ and C_{inh} to obtain free energy of adsorption ΔG_{ads}.

Table 2. Isotherms parameters for various temperatures

Isotherm	T(K)	R^2	Slope	Intercept
Langmuir	298	0.9992	1.0813	0.6435
	303	0.9996	1.1581	0.6819
	308	0.9997	1.2922	0.7645
	313	0.9997	1.4576	0.8567
	318	0.9998	1.7121	0.9100
	323	0.9996	1.8651	0.9784
Temkin	298	0.9949	0.1838	1.2307
	303	0.9977	0.2019	1.2244
	308	0.9904	0.2264	1.2080
	313	0.9951	0.1971	1.0617
	318	0.9865	0.1475	0.8638
	323	0.9880	0.1506	0.8292
El-Awady	298	0.9790	0.5294	1.8691
	303	0.9802	0.4943	1.6577
	308	0.9776	0.4686	1.6577
	313	0.9916	0.3630	1.4331
	318	0.9854	0.2586	0.6380
	323	0.9888	0.2638	0.5766
Freundlich	298	0.9928	0.1003	0.1365
	303	0.9999	0.1170	0.1676
	308	0.9965	0.1451	0.1676
	313	0.9987	0.1431	0.1101
	318	0.9947	0.1232	0.0009
	323	0.9940	0.1371	0.0037

A better understanding of the adsorption behaviour of an inhibitor can be obtained from thermodynamic adsorption parameters values. The free adsorption enthalpy (ΔG^0_{ads}) is calculated using the following relation [45]:

$$\Delta G^0_{ads} = -RTln(55.5K_{ads}) \qquad (5)$$

Where R is the perfect gas constant, T is absolute temperature and the constant 55.5 is the molar concentration of water. K_{ads} is the equilibrium constant of the adsorption process. The values of adsorption equilibrium constant are deduced from the parameters of the modified Langmuir isotherm (intercept of straight lines).

With regard to the other thermodynamic adsorption parameters, adsorption enthalpy (ΔH^0_{ads}) and adsorption entropy (ΔS^0_{ads}). They are calculated using the following relationship:

$$\Delta G^0_{ads} = \Delta H^0_{ads} - T\Delta S^0_{ads} \quad (6)$$

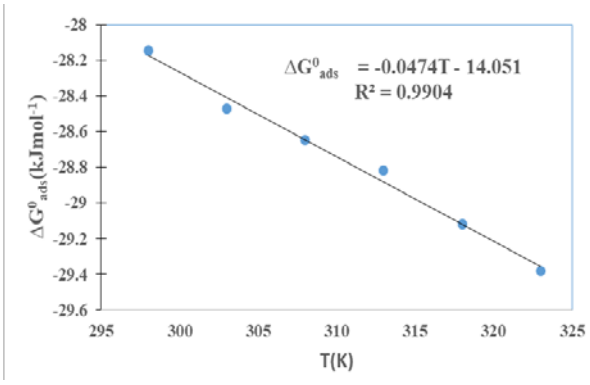

Figure 9. ΔG^0_{ads} versus temperature in the case of modified Langmuir isotherm

Plotting ΔG^0_{ads} versus temperature gives a straight line (Figure 9) whose slope and intercept permit to determine ΔS^0_{ads} and ΔH^0_{ads} respectively. The different thermodynamic adsorption parameters are recorded in Table 3.

Table 3. K_{ads} **and thermodynamic adsorption parameters for nifuroxazid**

T(K)	K_{ads}	ΔG^0_{ads} $(kJ\ mol^{-1})$	ΔH^0_{ads} $(kJ\ mol^{-1})$	ΔS^0_{ads} $(J\ mol^{-1}K^{-1})$
298	1554.0016	-28.1440	-14.054	47.4
303	1466.4907	-28.4703		
308	1308.0444	-28.6474		
313	1167.2698	-28.8163		
318	1098.9011	-29.1171		
323	1022.0769	-29.3804		

It can be clearly seen from Table 3 that $\Delta G^0_{ads} < 0$, this suggests that nifuroxazid is spontaneously adsorbed onto aluminium surface. Moreover ΔG^0_{ads} can be used to judge the absorption nature. In fact, when ΔG^0_{ads} values are between -20 kJ/mol and -40 kJ/mol, adsorption is both chemical and physical. ΔG^0_{ads} values obtained in this work fall within this range, indicating physisorption and chemisorption existence [47]. From the equation of the straight line, we deduce the values of change in adsorption enthalpy $\Delta H^0_{ads} = -14.054 kJ.mol^{-1}$ and that of change in adsorption entropy $\Delta S^0_{ads} = 47.4 J\ mol^{-1}K^{-1}$ .The negative sign of change in adsorption enthalpy indicates an exothermic adsorption process while the positive sign of ΔS^0_{ads} shows that disorder increases probably due to desorption of water molecules.

In order to identify the temperature ranges corresponding to each adsorption mode, Adejo-Ekwenchi isotherm [46] was used. This model is based on the following equation:

$$log\left(\frac{1}{1-\theta}\right) = log\ K_{AE} + b log C_{inh} \quad (7)$$

Where C_{inh} is the concentration of the adsorbate, K_{AE} and b are the isotherm parameters.

Figure 10 shows the representation of this isotherm. The parameters issued for this isotherm are listed in Table 4. It can be noted from Table 4 that b parameter values decrease from 298K to 318K, reflecting a physical adsorption process [48]. Whereas b values remain constant from 318K to 323K, indicating a chemical adsorption process [48].

Table 4. Parameters of the Adejo-Ekwenchi isotherm plots

T(K)	R^2	b	$logK_{AE}$	K_{AE}
298	0.9683	0.4291	1.7326	54.02564
303	0.9672	0.3773	1.5099	32.35191
308	0.9622	0.3235	1.2655	18.42892
313	0.9812	0.22	0.9207	8.33105
318	0.9864	0.1267	0.6146	4.11718
323	0.9795	0.1267	0.5803	3.80452

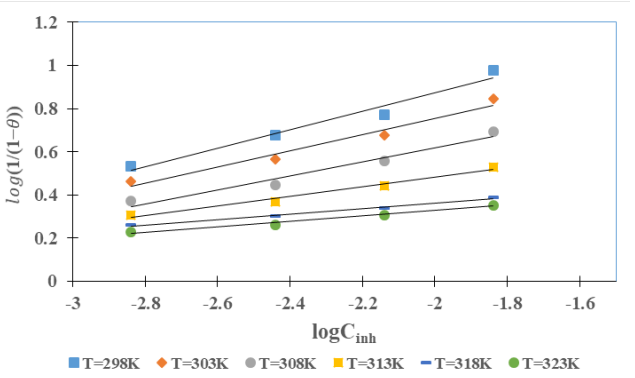

Figure 10. Plots of Adejo-Ekwenchi adsorption isotherm for nifuroxazid onto aluminium in 2.0M HCl

3.1.3. Effect of Temperature

The mass loss technique was used to examine temperature effect on corrosion rate and inhibition efficiency. This effect permits to determine corrosion activation energies in the absence and presence of inhibitor, as well as enthalpy and entropy activation. These kinetic and thermodynamic parameters of aluminium dissolution process are determined from Arrhenius equation (20) and transition state equation (21):

$$logW = logA - \frac{E_a}{2.3.R.T} \quad (8)$$

$$log\left(\frac{W}{T}\right) = log\left(\frac{R}{N_A.h}\right) + \frac{\Delta S^*_a}{2.3.R} - \frac{\Delta H^*_a}{2.3.R.T} \quad (9)$$

Where E_a is the apparent activation energy, R is the molar gas constant, k_0 is the frequency factor, h is the Planck's constant, N_A is the Avogadro number, ΔS^*_a is the change in activation entropy and ΔH^*_a is the change in activation enthalpy.

Figure 11 gives the plots of $logW$ versus $\frac{1}{T}$; the values of activation energy are obtained from the slopes of the straight lines. All the calculated parameters are listed in

Table 5. Figure 12 shows the plots of $log\left(\frac{w}{T}\right)$ versus $\frac{1}{T}$. The slopes and intercession of the straight lines obtained lead to the determination of entropy and enthalpy activation values respectively.

The high values of E_a and ΔH_a^* obtained in the presence of Nifuroxazid certifies that that aluminium dissolution becomes increasingly difficult as inhibitor concentration increases, confirming physisorption predominance [49,50]. This decrease in dissolution is linked to the gain of electrons that metal receives from inhibitor. ΔS_a^* values are positive in inhibitor presence, attesting that complex activated formation in the rate-determining step is dissociative rather than associative and can be interpreted as desorption of the absorbed species [50], resulting in increased disorder [51].

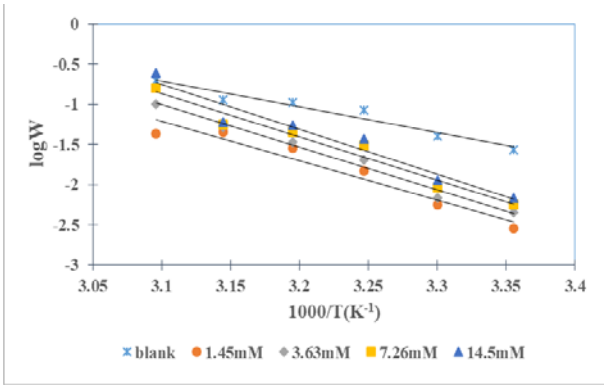

Figure 11. Arrhenius plots for the dissolution of aluminium in 2.0 M HCl without or with various concentrations of nifuroxazid

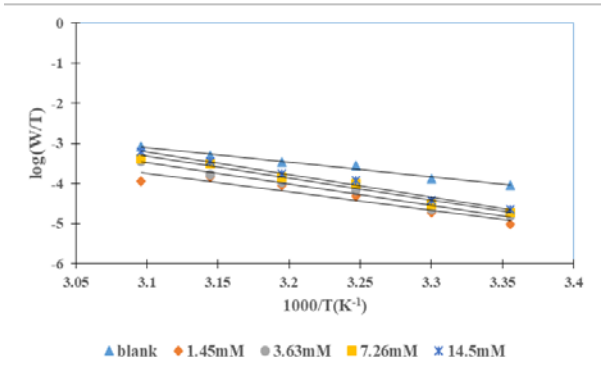

Figure 12. Transition state plots for aluminium dissolution in the absence and presence of various concentrations of nifuroxazid

Table 5. Dissolution parameters of aluminium in 1.0 M HCl without and with various concentrations of nifuroxazid

System/ Concentration	E_a $(kJ.mol^{-1})$	ΔH_a^* $(kJ.mol^{-1})$	ΔS_a^* $(J.mol^{-1}.K^{-1})$
Blank	61.290	69.867	- 40.675
1.45 mM	94.329	87.623	1.894
3.63 mM	101.195	101.708	50.653
7.26 mM	103.090	104.534	62.536
14.5 mM	106.882	108.068	75.721

3.2. Quantum Chemical Consideration (Interpretation)

3.2.1. Global Molecular Reactivity

Mass loss technique showed that nifuroxazid adsorbs to aluminium surface through chemical and physical interactions, thereby decreasing metal dissolution in 2M HCl. Quantum chemical parameters derived from DFT were solicited to explain the mechanism of this decrease. These parameters were calculated from DFT/6-31G(d, p) and are recorded in Table 6. This table examination, according to the literature, reports that E_{HOMO} value is high. This value indicates that nifuroxazid can donate electrons to aluminium [52,53,54]. As for E_{LUMO} value is low, indicating that inhibitor can receive electrons from metal [52,55]. Electron-donating and electron-receiving properties of nifuroxazid reinforce metal-molecule interactions. These interactions promote covalent bonds formation that help to create a protective film on aluminium surface. Density distribution of the inhibitor's molecular orbitals is shown in Figure 13, with HOMO orbital almost distributed over entire molecule surface and LUMO orbital partially distributed. These different distributions describe inhibitor reactivity. This reactivity also depends on the value of ΔE . Indeed, a low ΔE value indicates that the molecule is unstable, and the more readily it reacts with the metal to form coordination bonds. ΔE value obtained from the relationship $\Delta E = E_{LUMO} - E_{HOMO}$ indicates that nifuroxazid is reactive [56] and that the distribution as indicated by HOMO orbital confirms the predominance of its electron-donor character. Electron donor-acceptor properties are also confirmed by ionization potential (I) and electron affinity (A) values [57]. In fact, these two parameters I and A are linked by HOMO and LUMO energy respectively related through expressions $I = -E_{HOMO}$ and $A = -E_{LUMO}$. Absolute hardness $\left(\eta = \frac{I - A}{2}\right)$ and softness ($\sigma = \frac{1}{\eta}$) are very important parameters to describe molecular reactivity and stability [57]. Soft molecules are more reactive than hard ones because they can easily offer electrons. Hence, inhibitors with highest values of global softness σ the least values of the global hardness) are expected to be good corrosion inhibitor for bulk metals in acidic media. The calculations indicate our inhibitor have high softness values compared to the literature [58]. Fraction of transferred electrons determined from meta and molecule electronegativities is expressed as follows:

$\Delta N = \frac{\chi_{Al} - \chi_{inh}}{2\left(\eta_{Al} + \eta_{inh}\right)}$ with $\chi_{Al} = 4.28eV$ [59] et $\eta_{Al} = 0$ [59]. ΔN value is positive, certifies that aluminium can attract electrons from the inhibitor. This property enables nifuroxazid to replace the electrons lost by aluminium during oxidation. As far as dipole moment μ is concerned, there are many contradictions in the literature about the correlation between this parameter and inhibition efficiency [59,60], so no interpretation between two quantities can be made in this work. Molecule's ability to receive electrons from metal is confirmed by high value of Electrophilicity index (ω) [61].

Table 6. Global reactivity parameters of nifuroxazid by B3LYP/6-31G(d, p)

Global reactivity parameters	6-311G(d,p)
E_{HOMO} (eV)	-6.5585
E_{LUMO} (eV)	-2.8946
Energy gap ΔE (eV)	3.6639
Dipole moment μ (D)	6.9809
Ionization energy *I* (eV)	6.5585
Electron affinity *A* (eV)	2.8946
Electronegativity χ (eV)	4.7266
Hardness η (eV)	1.8320
Softness σ $(eV)^{-1}$	0.5458
fraction of electrons transferred ΔN	-0.1219
Electrophylicity index ω	6.0975
Total energy E_T (Ha)	-1003.1775035
CPU Temps de calcul	6 h 39 min 55.0 s

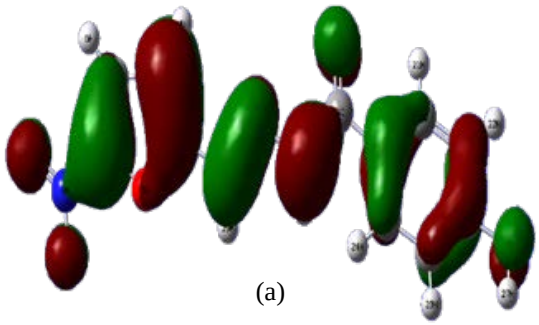

(a)

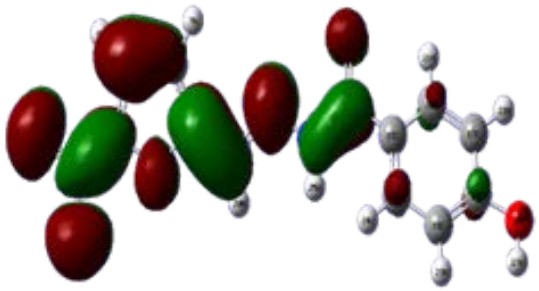

(b)

Figure 13. HOMO (a) and LUMO (b) of nifuroxazid by B3LYP/6-31G (d, p)

3.2.2. Correlation of Theoretical and Experimental Data

Theoretical reactivity descriptors interpretation indicates that nifuroxazid has both electron-donating and electron-accepting properties. These properties are due to the presence of oxygen atoms (O), nitrogen atoms (N) and π-bonds capable of ensuring electron exchange. In addition, the molecule is protonated in hydrochloric acid. At low temperatures, this creates a strong interaction between protonated species and the charged ions on metal surface.

Table 7. Calculated Mulliken atomic charges, Fukui functions and dual descriptor by DFT B3YLP6-31/G (d, p)

Atoms	$q_k(N+1)$	$q_k(N)$	$q_k(N-1)$	f_k^+	f_k^-	$\Delta f_k(\mathbf{r})$
1 C	0.204962	0.393904	0.062786	-0.188942	0.331118	-0.52006
2 C	-0.051256	-0.094922	0.025008	0.043666	-0.11993	0.163596
3 C	0.13113	-0.069536	-0.009597	0.200666	-0.059939	0.260605
4 C	0.065202	0.139085	0.09495	-0.073883	0.044135	-0.118018
5 O	-0.018698	-0.331376	0.065409	0.312678	-0.396785	0.709463
6 H	0.001429	0.147478	-0.001755	-0.146049	0.149233	-0.295282
7 H	-0.006684	0.143766	0.000146	-0.15045	0.14362	-0.29407
8 N	-0.020821	0.13126	0.101234	-0.152081	0.030026	-0.182107
9 O	0.038209	-0.220381	0.118268	0.25859	-0.338649	0.597239
10 O	0.00555	-0.307968	0.115036	0.313518	-0.423004	0.736522
11 C	0.064694	0.073599	0.047722	-0.008905	0.025877	-0.034782
12 N	0.072522	-0.159711	0.18158	0.232233	-0.341291	0.573524
13 N	0.208898	-0.278631	-0.034091	0.487529	-0.24454	0.732069
14 C	-0.024422	0.414784	0.067013	-0.439206	0.347771	-0.786977
15 C	0.135676	-0.180125	0.002078	0.315801	-0.182203	0.498004
16 C	-0.028351	-0.018782	0.043422	-0.009569	-0.062204	0.052635
17 C	0.058178	-0.080392	-0.022981	0.138570	-0.057411	0.195981
18 C	0.076264	0.168272	0.056349	-0.092008	0.111923	-0.203931
19 C	0.039736	-0.119847	-0.022701	0.159583	-0.097146	0.256729
20 C	-0.007343	-0.052019	0.041095	0.044676	-0.093114	0.13779
21 H	0.000683	0.12210	-0.002674	-0.121417	0.124774	-0.246191
22 H	-0.003315	0.125719	0.000981	-0.129034	0.124738	-0.253772
23 H	-0.002499	0.107904	0.001024	-0.110403	0.10688	-0.217283
24 H	-0.000394	0.094634	-0.001362	-0.095028	0.095996	-0.191024
25 H	-0.008541	0.205236	0.000034	-0.213777	0.205202	-0.418979
26 O	0.082440	-0.394680	0.006017	0.477120	-0.400697	0.877817
27 H	-0.002504	0.255607	-0.000183	-0.258111	0.25579	-0.513901
28 O	-0.007217	-0.320845	0.069967	0.313628	-0.390812	0.70444
29 H	-0.003528	0.105865	-0.004773	-0.109393	0.110638	-0.220031

This strong interaction permits the inhibitor to adsorb on aluminium surface via electrostatic bonds, which provide protection at low temperatures, justifying the high inhibition efficiencies obtained between 298K and 313K.

However, at high temperatures, aluminium loses many electrons, and the electrostatic bonds are destroyed by covalent bonds formation. These covalent bonds fail to establish a good protective layer on metal surface to reduce its high electron loss, as quantum parameters such as E_{LUMO}, ω mention that some of these lost electrons are donated to molecule. These data attest to the low inhibition efficiency values obtained at high temperatures. Despite the above, there is a good correlation between global quantum chemical parameters derived from DFT and the experimental results. Similar correlations have been reported in previous studies [62,63].

3.2.3. Local Molecular Reactivity

To get some insight into the local selectivity of the studied inhibitors, the Fukui functions are computed since they are the reactivity indicators of choice in the study of electron transfer controlled reactions such as corrosion inhibition process [64,65,66].

Calculated Fukui function and dual descriptor of nifuroxazid are presented in Table 7. These functions help to distinguish each part of the molecule according to its behaviour due to the different functional groups. Thus the site for nucleophilic attack will be the site where f_k^+ value and $\Delta f_k(r)$ are the highest values. While, electrophilic attack site is determined by the highest value f_k^- and the lowest value of $\Delta f_k(r)$. According to the literature, in case of ambiguity, the values of dual descriptors are used to indicate the sites of reactivities, because the dual descriptor is a more accurate local reactivity descriptor than Fukui functions [67]. Based on this information, 26 O is the most probable site to receive nucleophilic attacks while 14C is the most likely center for electrophilic attacks.

4. Conclusion

This study revealed the following key points:

- Nifuroxazid has good inhibition potential in 2M aluminum corrosion at low temperatures.
- Experimental results show that nifuroxazid inhibition efficiency increases with its concentration, but decreases as corrosive solution temperature rises.
- Inhibition efficiency reaches at a maximum value of 89,45% for 14.5mM concentration at 298K of temperature.
- Nifuroxazid adsorbs on aluminium surface according to Langmuir isotherm or Villamil model.
- Thermodynamic activation parameter values suggest that inhibition mechanism is influenced by physical adsorption.
- Local reactivity parameters indicate that atoms 26 O and 14C are the likely sites of nucleophilic and electrophilic attack respectively.

Quantum chemical calculations data from B3LYP/6-31G (d, p) are in good agreement with experimental results.

References

[1] Mahmood, D., Al-Okbi, A. K., Hanon, M. M., Rida, K.S., Alkaim, A. F., Al-Amiery, A. A., and Kadhum A.A., Carbethoxythiazole corrosion inhibitor: as an experimentally model and DFT theory, *Journal of Engineering and Applied Science*, 13(11). 3952–3959, 2018.

[2] Kadhim, A., Salim, E. T., Fayadh, S. M., Al-Amiery, A. A., Kadhum A. A. H. and Mohamad, A. B., Effect of Multipath Laser Shock Processing on Microhardness, Surface Roughness And Wear Resistance of 2024-T3 Al Alloy, *The Scientific World Journal*, 1–6. May 2014.

[3] Alobaidy, A., Kadhum, A., Al-Baghdadi, S., Al-Amiery, A.A., Kadhum A.A. H., Yousif, E. and Mohamad, A.B., Eco-friendly corrosion inhibitor: experimental studies on the corrosion inhibition performance of creatinine for mild steel in HCl complemented with quantum chemical calculations, *International Journal of Electrochemical Science*, 10(5). 3961–3972. May 2015.

[4] Junaedi, S., Kadhum A.A.H.,, Al-Amiery, A., Mohamad A.B., and Takriff, M.S., Synthesis and characterization of novel corrosion inhibitor derived from oleic acid: 2-Amino-5-Oleyl 1,3,4-Thiadiazol (AOT), *International Journal of Electrochemical Science*,7(4). 3543–3554. Apr. 2012.

[5] Lamghafria, S., Daoudi,W., El Aatiaoui, A., Dagdag, O., Berisha, A., Barrahi, A., Wan Nik, W.B., Zarrouk, A., Lahamdi, A., Comparative study of the performance and inhibitory efficiency of two new organic heterocyclic in the chemical industry, *Materials Science and Engineering: B*, 297. 116779. Nov.2023.

[6] Fouda, A.S., El Morsi M.A., & El Mogy, T., Studies on the inhibition of carbon steel corrosion in hydrochloric acid solution by expired Carvedilol drug, *Green Chemistry Letters and Reviews*, 10(4). 336-345. Oct. 2017.

[7] Ahamad, A., Khan, S., Ansari, K.R., Quraishi, M.A., Primaquine: A pharmaceutically active compound as corrosion inhibitor for mild steel in hydrochloric acid solution, *Journal of Chemical and Pharmaceutical Research*, 3(2). 703-717. 2011.

[8] Jamil D.M., Al-Okbi, A.K., Al-Baghdadi, S. B., Al-Amiery, A.A., Kadhim, A., Gaaz, T.S., Kadhum, A.A.H. and Mohamad, A.B., Experimental and theoretical studies of Schiff bases as corrosion inhibitors, *Chemistry Central Journal*, 12(1).1–9. Feb.2018.

[9] Ahmed, M.H.O., Al-Amiery, A.A., Al-Majedy, Y.K., Kadhum, A.A.H., Mohamad, A.B. and Gaaz, T.S., Synthesis and characterization of a novel organic corrosion inhibitor for mild steel in 1M hydrochloric acid, *Results in physics*. 8. 728-733. Mar. 2018.

[10] Abdulazeez, M.S., Abdullahe, Z. S., Dawood, M.A., Handel, Z. K., Mahmood, R.I., Osamah, S., Kadhum, A. A. H., Shaker, L.M. and Al-Amiery, A.A., Corrosion inhibition of low carbon steel in HCl medium using a thiadiazole derivative: mass loss, DFT studies and antibacterial studies, *International Journal of Corrosion and Scale Inhibition*, 10(4). 1812-1828, Dec.2021.

[11] Al-Amiery, A.A., Kadhim, A., Al-Adili, A. and Tawfiq, Z.H., Limits and developments in ecofriendly corrosion inhibitors of mild steel: a critical review. Part 1: Coumarins, *International Journal of Corrosion and Scale Inhibition*, 10(4). 1355–134, Sep.2021.

[12] Dawood, M.A., Alasady, Z. M. K., Abdulazeez, M.S., Ahmed, D. S., Sulaiman, G.M., Kadhum, A.A.H., Shaker L. M. and Alamiery, A.A., The corrosion inhibition effect of a pyridine derivative for low carbon steel in 1 M HCl Medium: Complemented with antibacterial studies, *International Journal of Corrosion and Scale Inhibition*, 10(4). 1766–1782. Dec. 2021.

[13] Salman, T.A., Zinad, D.S., Jaber, S.H., Shayaa, M., Mahal, A., Takriff, M.S. and Al-Amiery, A.A., Effect of 1,3,4-thiadiazole scafold on the corrosion inhibition of mild steel in acid medium: an experimental and computational study, *Journal of Bio-and Tribo-Corrosion*, 5. 48. Apr. 2019.

[14] Eddy, N.O., Ebenso, E.E., Adsorption and Quantum Chemical Studies on Cloxacillin and Halides for the Corrosion of Mild Steel in Acidic Medium, *International Journal of Electrochemical Science*, 5(6). 731-750. Jun.2010.

[15] Ahamad, I., Prasad, R., Quraishi, M.A., Inhibition of mild steel corrosion in acid solution by Pheniramine drug: Experimental and theoretical study, *Corrosion Science*, 52(9). 3033-3041. Sep.2010.

[16] Karthik, G., Sundaravadivelu M., Studies on the inhibition of mild steel corrosion in hydrochloric acid solution by atenolol drug, *Egyptian Journal of Petroleum*, 25(2).183-191. Jun.2016.

[17] Abdallah, M., Antibacterial drugs as corrosion inhibitors for corrosion of aluminium in hydrochloric solution, *Corrosion Science*, 46(8). 1981-1996. Aug.2004.

[18] Fouda, A.S., Al-Sarawy, A.A., Ahmed, F. S., & El-Abbasy, H.M., Corrosion inhibition of aluminum 6063 using some pharmaceutical compounds. *Protection of Metals and Physical Chemistry of Surfaces*, 45. 635-643. Sep.2009.

[19] Karthik, G., Sundaravadivelu, M., Inhibition of Mild Steel Corrosion in Sulphuric Acid Using Esomeprazole and the Effect of Iodide Ion Addition, *International Scholarly Research Notices*, 2013. 1-10. Feb.2013.

[20] Abdel Nazeer, A., El-Abbasy, H.M. & Fouda, A.S. Adsorption and Corrosion Inhibition Behavior of Carbon Steel by Cefoperazone as Eco-Friendly Inhibitor in HCl, *Journal of materials engineering and performance*, 22. 2314–2322. Apr.2013.

[21] Fayomi, O.S.I., Akande, I.G., Popoola, A.P.I., & Molifi, H., Potentiodynamic polarization studies of Cefadroxil and Dicloxacillin drugs on the corrosion susceptibility of aluminium AA6063 in 0.5 M nitric acid, *Journal of Materials Research and Technology*, 8(3). 3088-3096. May-Jun.2019.

[22] Rashid, K.H., Khadom, A.A., Abbas, S.H., Al-azawi, K.F., & Mahood, H.B., Optimization studies of expired mouthwash drugs on the corrosion of aluminum 7475 in 1 M hydrochloric acid: Gravimetrical, electrochemical, morphological and theoretical investigations, *Results in Surfaces and Interfaces*, 13.100165. Oct. 2023.

[23] Zarrouk, A., El Ouali, I., Bouachrine, M., Hammouti, B., Ramli, Y., Essassi, E. M., ... & Salghi, R., Theoretical approach to the corrosion inhibition efficiency of some quinoxaline derivatives of steel in acid media using the DFT method, *Research on Chemical Intermediates*, 39.1125–1133. Mar. 2013.

[24] El Hassani, A.A., El Adnani, Z., Benjelloun, A.T. Sfaira, M., Benzakour, M., Mcharfi, M., ... & Emran, K. M., DFT Theoretical Study of 5-(4-R-Phenyl)-1*H*-tetrazole (R = H; OCH_3; CH_3; Cl) as Corrosion Inhibitors for Mild Steel in Hydrochloric Acid, *Metals and Materials International*, 26.1725-1733. Nov.2020.

[25] Gece, G., & Bilgiç, S. Quantum chemical study of some cyclic nitrogen compounds as corrosion inhibitors of steel in NaCl media. *Corrosion Science*, 51(8). 876-1878. Aug.2009.

[26] Masoud, M.S., Awad, M.K., Ali, A.E., El-Tahawy, M.M.T., Molecular structure of amino alcohols on aluminum surface, *Journal of Molecular Structure*, 1063. 51-59. Apr.2014.

[27] Eddy, N.O., Momoh-Yahaya, H., & Oguzie, E. E., Theoretical and experimental studies on the corrosion inhibition potentials of some purines for aluminum in 0.1 M HCl, *Journal of Advanced Research*, 6(2). 203-217. Mar.2015.

[28] Khaled, K.F., Electrochemical investigation and modeling of corrosion inhibition of aluminium in molar nitric acid using somme sulphur containing amines, *Corrosion Science*, 52(9). 2905-2916. Sep. 2010.

[29] Gece, G., The use of quantum chemical methods in corrosion inhibitor studies, *Corrosion Science*, 50(11) .2981-2992. Nov2008.

[30] Chen, X., Tian, W., Li, S., Yu, M., Liu, J., Effect of temperature on corrosion behavior of 3003 aluminum alloy in ethylene glycol–water solution, *Chinese Journal of Aeronautics*, 29(4).1142-1150. Aug.2016.

[31] Obot, I.B., Macdonald, D.D., Gasem, Z.M., Density functional theory (DFT) as a powerful tool for designing new organic corrosion inhibitors, Part 1: An overview. *Corrosion Science*, 99. 1-30. Oct. 2015.

[32] MJ Frisch; GW Trucks; HB Schlegel; GE Scuseria; MA Robb; JR Cheeseman; G Scalmani; V Barone; B Mennucci; GA Petersson; H Nakatsuji; M Caricato; X Li; HP Hratchian; AF Izmaylov; J Bloino; G Zheng; JL Sonnenberg; M Hada; M Ehara; K Toyota; R Fukuda; J Hasegawa; M Ishida; T Nakajima; Y Honda; O Kitao; H Nakai; T Vreven; JA Montgomery; Jr., JE Peralta; F Ogliaro; M Bearpark; JJ Heyd; E Brothers; KN Kudin; VN Staroverov; R Kobayashi; J Normand; K Raghavachari; A Rendell; JC Burant; SS Iyengar; J Tomasi; M Cossi; N Rega; JM Millam; M Klene; JE Knox; JB Cross; V Bakken; C Adamo; J Jaramillo; R Gomperts; RE Stratmann; O Yazyev; AJ Austin; R Cammi; C Pomelli; JW Ochterski; RL Martin; K Morokuma; VG Zakrzewski; GA Voth; P Salvador JJ Dannenberg; S Dapprich; AD Daniels; Ö Farkas; JB Foresman; JV Ortiz; J Cioslowski; DJ Fox. Gaussian 09 (Gaussian, Inc., Wallingford CT). 2009.

[33] Becke, D., Density functional calculations of molecular bond energies, *The Journal of Chemical Physics*, 84. 4524-4529. Apr.1986.

[34] Lee, C.,Yang, W., Parr, R.G., Development of the Colle-Salvetti correlation-energy formula into a functional of the electron density, *Physical Review B*., 37. 785. Jan.1988.

[35] Mohamedien, H.A., Kamal, S.M., Taha, M., EL-Deeb, M.M., El-Deen, A.G., Experimental and computational evaluations of cefotaxime sodium drug as an efficient and green corrosion inhibitor for aluminum in NaOH solution, *Materials Chemistry and Physics* 290(15). 126546. Oct. 2022.

[36] Beda R.H.B., Tigori, M.A., Diabaté, D. and Niamien, P.M., Anticorrosive Properties of Theophylline on Aluminium Corrosion in 1 M HCl: Experimental, and Computational Assessment of Iodide Ions Synergistic Effect. *Current Physical Chemistry*, 11(3). 227-242. Nov.2021.

[37] Obot, I.B., and Obi-Egbedin, N.N., Inhibitory effect and adsorption characteristics of 2,3-diaminonaphthalene at aluminum/ hydrochloric acid interface: experimental and theoretical study, *Surface Review and Letters*, 15 (6) 903–910, Apr.2008.

[38] Abdallah, M., Hawsawi, H., Al-Gorair, A.S., Alotaibi, M.T., Al-Juaid S.S., Abdel Hameed, R.S., Appraisal of Adsorption and Inhibition Effect of Expired Micardis Drug on Aluminum Corrosion in Hydrochloric Acid Solution, *InternationalJournal of Electrochemical Science*,17(4) 220462, Apr. 2022.

[39] Dibetsoe, M., Olasunkanmi, L.O., Fayemi, O.E., Yesudass, S., Ramaganthan, B., Bahadur, I., ... & Ebenso, E.E. Some phthalocyanine and naphthalocyanine derivatives as corrosion inhibitors for aluminium in acidic medium: Experimental, quantum chemical calculations, QSAR studies and synergistic effect of iodide ions. *Molecules*, 20(9). 15701-15734. Aug. 2015.

[40] Deng, S., Li, X., Inhibition by Jasminum nudiflorum Lindl. leaves extract of the corrosion of aluminium in HCl solution, *Corrosion Science*, 64. 253-262. Nov. 2012.

[41] Temkin, M.I., Adsorption equilibrium and process Kinetics on inhomogeneous surfaces with interaction between adsorbed molecules, *Zhurnal Fizicheskoi Khimii*, 15(3). 296-332. 1941.

[42] El Awady, Y.A., Ahmed, A.I., Effect of temperature and inhibitors on the corrosion of aluminium in 2N HCl solution, A kinetic study, *Journal of Indian Chemistry*, 24A. 601-606. Jul.1985.

[43] Langmuir, I., the constitution and fundamental properties of solids and liquids, *Journal of the American Chemical Society*, 38(11). 2221-2295. Nov.1916.

[44] Villamil, R.F., Corio, P., Agostinho, S.M., & Rubim, J.C., Effect of sodium dodecylsulfate on copper corrosion in sulfuric acid media in the absence and presence of benzotriazole, *Journal of Electroanalytical chemistry*, 472(2). 112-119. Aug.1999.

[45] Vashi, R.T., Champaneri, V.A., Toluidines as corrosion inhibitors for zinc in sulphamic acid, *Indian Journal of Chemical Technology*, 4.180-184. Jul.1997.

[46] Adejo, S.O., Ahile, J.U., Gbertyo, J.A., Kaior, A., & Ekwenchi, M. M., Resolution of adsorption characterisation ambiguity through the Adejo-Ekwenchi adsorption isotherm: a case study of leaf extract of Hyptis suaveolen poit as green corrosion inhibitor of corrosion of mild steel in 2 M HCl. *Journal of Emerging Trends in Engineering and Applied Sciences*, 5(8). 201-205. Jan.2014.

[47] Benabdellah, M., Touzani, R., Dafali, A., Hammouti, B., & El Kadiri, S., Ruthenium–ligand complex, an efficient inhibitor of steel corrosion in H3PO4 media. *Materials Letters*, 61(4-5). 1197-1204. Feb. 2007.

[48] Adejo, S.O., Proposing a new empirical adsorption isotherm known as Adejo-Ekwenchi isotherm, *Journal of Applied Chemistry*, 6(5). 66-71. Jan. 2014.

[49] Boudalia, M., Sebbar, N. K., Bourazmi, H., Lahmidi, S., Ouzidan, Y., Essassi, E. M., Zarrouk, A., Anti-corrosive properties of new Benzothiazine derivative on mild steel corrosion in 1 M HCl: Experimental and theoretical investigations. *Journal of Materials and Environmental Science*, 7(3). 878-888. Sep. 2016.

[50] Obi-Egbedi, N.O., & Obot, I.B., Inhibitive properties, thermodynamic and quantum chemical studies of alloxazine on mild steel corrosion in H_2SO_4. *Corrosion Science*, 53(1). 263-275. Jan. 2011.

[51] Adejoro, I. A., Ibeji, C.U., & Akintayo, D.C., Quantum descriptors and corrosion inhibition potentials of Amodiaquine and Nivaquine. *Chemical Sciences Journal*, 8. 149. Jan. 2017.

[52] Damej, M., Kaya, S., Lee, H-S., Molhi, A., Serdaroğlu, G., Benmessaoud, M., Ali, I.H., El Hajjaji, S., Lgaz, H., The corrosion inhibition and adsorption behavior of mercaptobenzimidazole and bis-mercaptobenzimidazole on carbon steel in 1.0 M HCl: Experimental and computational insights, *Surfaces and Interfaces*, 24. 101095. Jun. 2021.

[53] Özcan, M., Toffoli, D., Üstünel, H., & Dehri, I., Insights into surface–adsorbate interactions in corrosion inhibition processes at the molecular level. *Corrosion science*, 80. 482-486. Mar.2014.

[54] Obi-Egbedi, N. O., Obot, I. B., & El-Khaiary, M. I. Quantum chemical investigation and statistical analysis of the relationship between corrosion inhibition efficiency and molecular structure of xanthene and its derivatives on mild steel in sulphuric acid. *Journal of Molecular Structure*, 1002(1-3). 86-96. Sept.2011.

[55] Ahamad, I., Prasad, R., & Quraishi, M.A., Adsorption and inhibitive properties of some new Mannich bases of Isatin derivatives on corrosion of mild steel in acidic media, *Corrosion Science*, 52(4). 1472-1481. Jan.2010.

[56] Al Jahdaly, B. A., Rosmarinus officinalis extract as eco-friendly corrosion inhibitor for copper in 1 M nitric acid solution: Experimental and theoretical studies, *Arabian Journal of Chemistry*, 16(1). 104411. Jan. 2023.

[57] Niamien, P.M., Essy, F.K., Trokourey, A., Yapi, A., Aka, H.K., Diabate, D., Correlation between the molecular structure and the inhibiting effect of some benzimidazole derivatives, *Materials Chemistry and Physics*, 136(1). 59-65. Sep. 2012.

[58] Yeo, M., Niamien, P.M., Bilé, E.B.A., & Trokourey, A., Thiamine hydrochloride as a potential inhibitor for aluminium corrosion in 1.0 M HCl: mass loss and DFT studies. *Journal of Computational Methods in Molecular Design*, 7. 13-25. 2017.

[59] Lagrenée, M., Mernari, B., Chaibi, N., Traisnel, M., Vezin, H., Bentiss, F., Investigation of the inhibitive effect of substituted oxadiazoles on the corrosion of mild steel in HCl medium, *Corrosion Science*, 43(5). 951-962. May 2001.

[60] R.G. Pearson. Absolute electronegativity and hardness: application to inorganic chemistry, *Inorganic Chemistry*, 27. 734-740. Feb.1988.

[61] Parr, R.G., Sventpaly, L., & Liu, S. Electrophilicity index. *Journal of the American Chemical Society*, 121(9). 1922-1924. Feb.1999.

[62] Id El Mouden, O., Belghiti, M.E., Mizeb, K., El Ghozlani, M., Matine, A., Batah, A., ... & Elalaoui-Elabdallaoui, H., Anti-corrosive properties of two new green heterocyclic azole derivatives on C38 steel in 1 M (HCl) medium, experimental and theoretical study, *Results in Chemistry*, 5. 100641. Jan. 2023.

[63] Bashir, S., Sharma, V., Singh, G. et al., Electrochemical Behavior and Computational Analysis of Phenylephrine for Corrosion Inhibition of Aluminum in Acidic Medium, *Metallurgical and Materials Transactions A*, 50. 468–479. Jan. 2019.

[64] Rodríguez-Valdez, L.M., Villamisar,W., Casales, M., Gonzalez-Rodriguez, J.G., Martínez-Villafañe, A., Martinez, L., & Glossman-Mitnik, D., Computational simulations of the molecular structure and corrosion properties of amidoethyl, aminoethyl and hydroxyethyl imidazolines inhibitors, *Corrosion Science*, *48*(12). 4053-4064. Dec. 2006.

[65] Ayers, P.W., & Parr, R.G., Variational principles for describing chemical reactions: the Fukui function and chemical hardness revisited. *Journal of the American Chemical Society*, 122(9). 2010-2018. Feb.2000.

[66] Ayers, P.W., & Parr, R.G., Local hardness equalization: Exploiting the ambiguity, *The Journal of chemical Physics*, 128.184108. May 2008.

[67] Martínez-Araya, J.I., Why is the dual descriptor a more accurate local reactivity descriptor than Fukui functions? *The Journal of Mathematical Chemistry*, 53. 451–465 Oct.2015.